competent state of methane monooxygenase has been a driving force for developing the quantitative aspects of integer-spin EPR. The results obtained here indicate that EPR of integer-spin systems can be used to determine spin and zero-field splitting parameters and to provide an accurate determination of spin concentrations.

The EPR spectra reported here are typical of those observed for integer-spin complexes with large zero-field splittings. Spectra obtained in frozen solution exhibit rather broad features with line shapes dominated by distributions of zero-field parameters. The splitting of the EPR active doublet $\Delta(D,E)$ is also spread and the spread tends to straddle the X-band microwave energy. The resonance condition, eq 8, can only be satisfied for $\Delta < h\nu \approx 0.3$ cm^{-1}, thus, only a fraction of the molecular distribution is observed. Consequently, the success of spin quantitation depends on our ability to find the correct distributions for D and E, to allow a prediction of the fraction of molecules with $\Delta < h\nu$. The work described here shows that the spin concentration can be determined with good accuracy. While we are confident that such quantitation can be obtained for many other systems, we consider it advisable to study more systems where the results can be checked with a powerful technique such as Mössbauer spectroscopy. With more experience, it should be possible to venture with more confidence to systems such as Ni^{II} or Mn^{III} where EPR may have to stand on its own.

Substantial information of the spin system in question can be added by extending measurements to multifrequency EPR.[4a] Studies at additional frequencies not only give a cross-check of the parameters obtained at X-band, but in many cases it may be possible to observe additional resonances from a different pair of levels or from a species that is EPR silent at X-band. As an example consider complex **1**. Figure 8 shows a plot of the probability distribution of Δ values for the $|3,0\rangle$, $|3,1^-\rangle$ pair (solid line) computed from the distributions of D and E used for the simulations of Figure 7. The vertical line at 0.3 cm^{-1} corresponds to the X-band microwave energy, i.e. only molecules with $\Delta <$ 0.3 cm^{-1} (left of line) contribute to the $g = 12$ resonance; the fraction is ≈50%. On the other hand, at Q-band (vertical line at 1.2 cm^{-1}) all molecules of the sample would be EPR active. Now consider the lowest pair of levels from the excited $S = 2$ quintet (see Figure 2) of complex **1**. The probability distribution of Δ values for the $|2,0\rangle$, $|2,1^-\rangle$ pair ($g_{eff} \approx 8$) is shown in Figure 8 (dashed line) as computed from the same parameter set. As mentioned above, only a small fraction of molecules is observed at X-band, whereas Q-band spectroscopy would show signals from virtually the entire molecular population.

Acknowledgment. We thank Prof. Oren Anderson and Kevin Andersen for their generous help in solving the structure of the FeCu complex. We are grateful to Prof. J. D. Lipscomb for allowing us frequent use of his EPR instrument. This work was supported by the National Institute of Health through Grants GM-38767 (L.Q.) and GM-22701 (E.M.), predoctoral traineeship GM-08277 (T.R.H.), and postdoctoral fellowship GM-12996 (M.P.H.).

Models of Lysine–Cysteine Hydrogen Bonding in Metallothionein: Hydrogen Bonding between Ammonium and Benzenethiolate in $[(C_6H_{11})_2NH_2]_2[Co(SC_6H_5)_4]$

Wesley P. Chung, John C. Dewan, and M. Anton Walters*

Contribution from the Department of Chemistry, New York University, New York, New York 10003. *Received May 7, 1990*

Abstract: Anion–cation hydrogen bonding interactions are described for $[(C_6H_{11})_2NH_2]_2[M(SC_6H_5)_4]$ where M = Co (**1**), Zn (**3**), which serve as models of putative lysine–cyteine hydrogen bonding at the metal binding site of metallothionein. Complex **1** is isolated as green crystals in which an average N–H···S hydrogen bond length of 3.29 (1) Å is observed in infinite one-dimensional chains. The dicyclohexylammonium counterion occupies a bridging position by hydrogen bonding to thiolate ligand sulfur atoms on adjacent anion complexes. There are two $[Co(SC_6H_5)_4]^{2-}$ anions per asymmetric unit where each Co atom is tetrahedrally coordinated by four benzenethiolate ligands [Co–S_{av} = 2.308 (4) Å]. In the non-hydrogen bonding complex $[(CH_3)_4N]_2[Co(SC_6H_5)_4]$ (**5**), a split vibrational band at 228 cm^{-1} (av) is assigned to a Co–S T_2 related mode. In $[(CH_3)_4N]_2[Zn(SC_6H_5)_4]$ (**7**) this band is replaced by one at 199 cm^{-1}. Relatively intense bands at 192 and 180 cm^{-1} in the Raman spectra of **1** and **3** are assigned to metal–ligand modes. Hydrogen bonding causes a decrease in metal–ligand bond length of 0.02 Å relative to the bonds in a non-hydrogen bonding complex.

Introduction

In the Zn- or Cd-containing forms of metallothionein (MT) metal ions are coordinated exclusively by cysteine (Cys) ligands in two binding sites M_4–Cys_{11}^{3-} and M_3–Cys_9^{3-}, designated α and β.[1] The coordination geometry of each metal ion is approximately tetrahedral.[1] There are seven positions along the polypeptide chain of MT where Cys and lysine (Lys) are adjacent. This has been considered to be of possible importance in the structure and stability of the metal binding sites of the protein. Vasak and co-workers[2,3] reported an unusually high pK_a for the Lys side chains. Demetalation of the protein in acidic solution caused a decrease in the Lys pK_a from 10.9 to 10.3. The deprotonation of Lys caused changes in the circular dichroism spectrum of the protein which were attributed to electrostatically induced structural alterations. In addition, the arylation of Lys by trinitrobenzenesulfonic acid resulted in changes in the CD spectrum of Cd–MT. The metal-free *S*-carboxamidomethyl derivative of MT had an average pK_a of 10.3 which differs from the value of 10.9 measured in the native protein. Taken together, these effects were argued to be consistent with the interruption of hydrogen bonds between Cys and Lys. It was suggested that hydrogen bonding to the cationic Lys side chain might serve to stabilize the met-

(1) Furey, W. F.; Robbins, A. H.; Clancy, L. L.; Winge, D. R.; Wang, B. C.; Stout, C. D. *Science (Washington, D.C.)* **1986**, *231*, 704–710.
(2) Vasak, M.; McClelland, Ch. E.; Hill, H. A. O.; Kagi, J. H. R. *Experientia* **1985**, *41*, 30–34.
(3) Pande, J.; Vasak, M.; Kagi, J. H. R. *Biochemistry* **1985**, *24*, 6717–6722.

0002-7863/91/1513-525$02.50/0

al–thiolate clusters of MT by delocalizing the net charge of 3– on each of the Zn,Cd–S sites.[2,3] This is similar to the situation in ferredoxins and rubredoxins, where hydrogen bonding between metal-coordinated Cys and peptide backbone amide has been considered as a possible modulator of redox potential.[4]

We have undertaken a study of N–H···S hydrogen bonding in metal–thiolate complexes and report here the first detailed study of ammonium–thiolate hydrogen bonds in tetrahedral $M(SC_6H_5)_4^{2-}$ model complexes. Our results show clear evidence for the formation of relatively strong N–H···S hydrogen bonds between alkylammonium counterions and coordinated benzenethiolate ligands in a transition-metal complex. On the basis of X-ray crystallographic data, it appears that hydrogen bond formation stabilizes these metal complexes. This represents the first proof of a definitive influence of hydrogen bonding on the structure of a metal–thiolate complex. From this data it is possible to infer the importance of hydrogen bonding to cysteine ligands in metal binding proteins both from the point of view of stability, in general, and redox potential, in the case of electron-transfer proteins.

Experimental Section

All procedures were carried out in an inert atmosphere glovebox or by Schlenk line methods.

Synthesis of $[(C_6H_{11})_2NH_2]_2[Co(SC_6H_5)_4]$ (1). Dicyclohexylamine (2.53 g, 13.9 mmol) and benzenethiol (1.54 g, 13.9 mmol) were dissolved in methanol to which cobalt(II) chloride hexahydrate (0.65 g, 2.73 mmol) was added, and the resulting green solution was stirred for 0.5 h. The product was concentrated to a paste and redissolved in approximately 25 mL of THF and filtered to remove $[(C_6H_{11})_2NH_2]Cl$. The filtrate was concentrated under vacuum to a volume of 5–10 mL, and crystallization was induced by the slow addition of ether by vapor diffusion. Dark green crystals formed overnight in a black solution which was poured off, and the crystals were dried under a stream of nitrogen. The product was dissolved in a minimum amount of CH_3CN at 50 °C and obtained as lustrous dark green needles on cooling the solution to room temperature (yield 1.3 g, 55%). For X-ray crystallography, the product was obtained as green needles from CH_3CN by slow evaporation of the solvent under vaccum. Elemental analysis was carried out by Galbraith Laboratories. Anal. Calcd for $C_{48}H_{68}CoN_2S_4$: C, 67.05; H, 7.91; Co, 6.87; N, 3.26; S, 14.90. Found: C, 67.73; H, 7.74; Co, 6.87; N, 3.28; S, 15.14.

Synthesis of $[(C_6H_{11})_2ND_2]_2[Co(SC_6H_5)_4]$ (2). Crystals of **1** (0.113 g) were dissolved in deuterated methanol, CH_3OD, 1 mL, under an inert atmosphere and stirred for 30 min. The methanol was removed by evaporation under vacuum, and the process was repeated.

Synthesis of $[(C_6H_{11})_2NH_2]_2[Zn(SC_6H_5)_4]$ (3). Sodium benzenethiolate (2.29 g, 17.3 mmol) and anhydrous zinc chloride (0.47 g, 3.46 mmol) were dissolved in methanol, 40 mL, resulting in the formation of a finely divided white precipitate. The solvent was removed by evaporation under vacuum and replaced by 40 mL of CH_3CN. Dicyclohexylammonium chloride (1.88 g, 8.65 mmol) was added, and the mixture was allowed to stir overnight. The solution was filtered to remove NaCl, and the filtrate was cooled to 0 °C to initiate crystallization. After 1.5 h, the product was isolated by decanting the solution, washed with ether, and vacuum dried (yield 0.94 g, 31%). Anal. Calcd for $C_{48}H_{68}N_2S_4Zn$: C, 66.52; H, 7.91; N, 3.23. Found: C, 66.26; H, 7.76; N, 3.20.

Syntheses of $[(C_6H_5)_4P]_2[Co(SC_6H_5)_4]$, $[(C_2H_5)_4N]_2[Co(SC_6H_5)_4]$, and $[(CH_3)_4N]_2[M(SC_6H_5)_4]$ (M = Fe (4), Co (5), Ni (6), and Zn (7)). These complexes were synthesized by methods slightly modified from those of Hagen et al.[5] and Rosenfield et al.[6] Analogous complexes containing *p*-thiocresolate ligands, $[(CH_3)_4N]_2[M(SC_6H_4CH_3)_4]$ (M = Co (**8**) and Zn (**9**), respectively), were synthesized by the same methods. Products were characterized by ^1H NMR,[5,6] electronic absorption[7] or infrared spectroscopy.[8]

Synthesis of $[(C_6H_{11})_2NH_2]Cl$ (10). A slight molar excess of concentrated HCl solution was added to a methanol or ether solution of dicyclohexylamine to form the amine hydrogen chloride. The product was obtained as a white amorphous solid after evaporation of the solvent. When methanol was used, the product was dried by heating to 50 °C under vacuum for approximately 1 h.

Methanol, acetonitrile, ether, and benzenethiol were distilled and stored under nitrogen before use. *p*-Thiocresol was purchased from Aldrich and recrystallized from heptane before use. Dicyclohexylamine was purchased from Aldrich and used without further purification.

Proton NMR data were acquired by using a General Electric QE 300 (300 MHz) spectrometer. CH_3CN-d_3 was used for all NMR experiments.

Samples were prepared in an inert atmosphere glovebox as KBr pellets for mid-IR and as mineral oil mulls for far-IR experiments. Mid-IR data were obtained at 4-cm^{-1} resolution by using a Nicolet 5DXB FTIR spectrometer. The FTIR sample chamber was purged with dry air. No sample decomposition was observed during the course of data collection which was typically complete within 20 min. Far-infrared data were acquired by using a Nicolet 20F FTIR spectrometer at 4-cm^{-1} resolution. Mulls were enclosed in a sealed cell with polyethylene windows. Both spectrometers were controlled by a Nicolet 1280 computer.

Raman data were obtained on samples prepared as mineral oil mulls in a coaxial 5-mm o.d. spinning NMR tube. A Coherent 70-4 Ar^+ laser operating at 10–20 mW was used as a radiation source. A SPEX 1401 monochromator set for 10-cm^{-1} spectral band pass with a SPEX R928-07 photomultiplier tube was used for the detection of Raman scattered light. Data were collected digitally by using an Anaheim Automation driver pack for monochromator stepper motor control and an EG&G Ortec ACE-MCS card and emulation software for photon counting. The monochromator was advanced in 1-cm^{-1} increments, with collection times of 1 s/point. Data were processed by using Galactic Industries SPECTRA CALC software.

Electronic absorption spectra were obtained by using a Perkin-Elmer Lambda 2 UV–vis spectrometer. During data collection the samples were exposed to air as KBr pellets for approximately 10 min. No decomposition was observed during that time.

X-ray Structure of $[(C_6H_{11})_2NH_2]_2[Co(SC_6H_5)_4]$ (1). X-ray data were collected at −120 °C on a Rigaku AFC-6S diffractometer equipped with a liquid-nitrogen low-temperature device using Mo Kα radiation. Details of data collection, reduction, and refinement procedures have been described elsehwere.[9] An absorption correction was applied by using the program DIFABS. A total of 16719 reflections ($+h,\pm k,\pm l$) were collected in the range $4° < 2\theta < 50°$. Of these 6573 had $I_o > 3\sigma(I_o)$ and were used in the structure solution and refinement, the latter being carried out by full-matrix least-squares techniques (491 variables) with the TEXSAN package of crystallographic programs from Molecular Structure Corporation. Three intensity standards decayed by 5.1%, and the data were corrected for this. Final $R_1 = 0.081$ and $R_2 = 0.091$. Hydrogen atoms were included in calculated positions, and the Co and S atoms were refined anisotropically. The final difference-Fourier map showed no significant features. Large crystals of **1** were twinned although a very small untwinned crystal, too small for data collection, gave the triclinic unit cell listed below. A larger crystal selected for data collection was twinned, but the MSC/Rigaku diffractometer control software was able to extract the same unit cell obtained for the small untwinned crystal. Data collection was carried out by using this larger crystal, but the final *R* values reflect the poor quality of the available crystals. Crystal data are as follows: $a = 16.989$ (10) Å, $b = 23.877$ (10) Å, $c = 11.918$ (8) Å, $\alpha = 97.96$ (4)°, $\beta = 97.05$ (5)°, $\gamma = 93.09$ (4)°, $V = 4739$ (5) Å^3, space group $P\bar{1}$, $Z = 4$, mol wt = 856.2 g, ρ(calcd) = 1.200 g cm^{-3}, μ = 5.61 cm^{-1}.

Table I. Hydrogen Bond Distances (Å)[a]

atoms	distance	atoms	distance
S(1)···N(1)	3.25 (1)	S(5)···N(3)	3.295 (9)
S(2)···N(1)′	3.27 (1)	S(6)···N(3)′	3.30 (1)
S(3)···N(2)	3.34 (1)	S(7)···N(4)	3.27 (1)
S(4)···N(2)′	3.29 (1)	S(8)···N(4)′	3.287 (9)

[a] Primed atoms and their unprimed counterparts are related by an inversion operation.

Results and Discussion

Crystal Structure. The structure of **1** consists of $[Co(SC_6H_5)_4]^{2-}$ anions and $[(C_6H_{11})_2NH_2]^+$ cations in a 1:2 ratio. In each asymmetric unit there are two independent anions (Figure 1a) and four independent cations. Anions are linked, via hydrogen-bonding interactions by bridging dicyclohexylamine cations, in infinite one-dimensional chains (Figure 1b). The hydrogen-bonding interactions occur between the N–H moieties of the cation

(4) Sheridan, R. P.; Allen, L. C. *Chem. Phys. Lett.* **1980**, *69*, 600–604.
(5) Hagen, K. S.; Reynolds, J. G.; Holm, R. H. *J. Am. Chem. Soc.* **1981**, *103*, 4054–4063.
(6) Rosenfield, S. G.; Armstrong, W. H.; Mascharak, P. K. *Inorg. Chem.* **1986**, *25*, 3014–3018.
(7) Dance, I. G. *J. Am. Chem. Soc.* **1979**, *101*, 6264–6273.
(8) Ueyama, N.; Sugawara, T.; Sasaki, K.; Nakamura, A.; Yamashita, S.; Wakatsuki, Y.; Yamazaki, H.; Yasuoka, N. *Inorg. Chem.* **1988**, *27*, 741–747.
(9) Young, A. C. M.; Walters, M. A.; Dewan, J. C. *Acta Crystallogr.* **1989**, *C45*, 1733–1736.

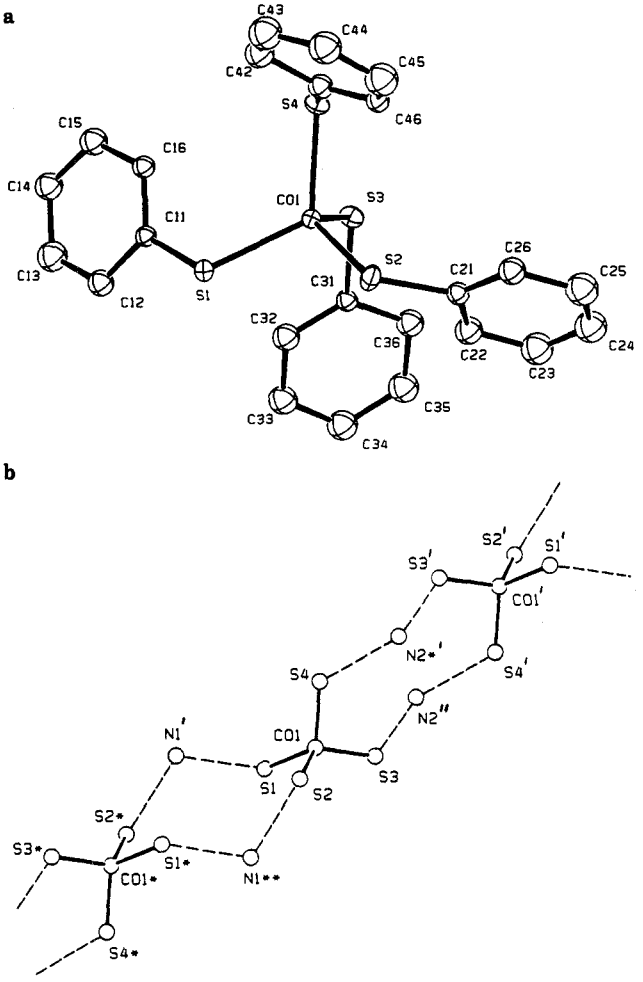

Figure 1. (a) ORTEP diagram of one of the $[Co(SC_6H_5)_4]^{2-}$ anions in **1** showing the atom labeling scheme and 30% probability thermal ellipsoids. (b) Diagram of one of the infinite one-dimensional chains of the structure formed by hydrogen-bonding interactions between the dicyclohexylamine cations and $[Co(SC_6H_5)_4]^{2-}$ anions. There is a center of symmetry between each pair of Co atoms. The symmetry code is as follows: * $(-x, -y, -z)$, ' $(1-x, -y, -z)$, ** $(-1+x, y, z)$, '' $(1-x, -y, 1-z)$, *' $(x, y, -1+z)$.

and the S atoms of the anion. All N–H groups and S atoms of the structure are involved in hydrogen-bonding interactions. The average distance between dicyclohexylammonium nitrogen and thiolate sulfur is 3.29 (1) Å (Table I), characteristic of relatively strong N–H···S hydrogen bonds with N–H donors. The range of values for such interactions is typically 3.3–3.5 Å.[10]

The individual complex anions in the asymmetric unit of **1** have four S–Co–S angles averaging 115.3 (1)° and two S–Co–S angles averaging 98.4 (1)°. This corresponds to local D_{2d} symmetry, which is similar to the structure reported by Swenson et al.[11] which has corresponding angles of 116.4 (2)° and 96.3 (2)°. The positions of the phenyl rings give an overall symmetry of D_2 to the anions of **1**.

In each anion the Co(II) ion is coordinated by four $(SC_6H_5)^-$ ligands in an approximately tetrahedral arrangement. The average Co–S distance is 2.308 (4) Å in each complex, slightly shorter than the average distance of 2.328 (4) Å reported for $[(C_6H_5)_4P]_2[Co(SC_6H_5)_4]$[11] (Table II). This is consistent with a net stabilization of the anionic cobalt complex. Such an effect apparently involves a shift of electron density from orbitals on sulfur to those of the hydrogen-bonded ammonium counterion. The monodentate thiolate ligand provides σ and π donation with the lone pair electrons occupying the sulfur π orbitals.[12] The latter may qualitatively be expected to contribute largely as antibonding orbitals, destabilizing the metal d and p orbitals.[13] Hydrogen bonding to sulfur might decrease the metal–sulfur π-interaction thereby stabilizing the metal–thiolate complex.

Table II. Selected Bond Distances (Å) and Bond Angles (deg) for $[Co(SC_6H_5)_4]^{2-}$ Anions

Selected Atomic Distances (Å)

atoms	distance	atoms	distance
	$[(C_6H_{11})_2NH_2]_2[Co(SC_6H_5)_4]$[a]		
Co(1)–S(1)	2.302 (4)	S(1)–C(11)	1.77 (1)
Co(1)–S(2)	2.321 (4)	S(2)–C(21)	1.77 (1)
Co(1)–S(3)	2.295 (4)	S(3)–C(31)	1.79 (1)
Co(1)–S(4)	2.311 (4)	S(4)–C(41)	1.78 (1)
Co(2)–S(5)	2.310 (4)	S(5)–C(51)	1.75 (1)
Co(2)–S(6)	2.304 (4)	S(6)–C(61)	1.77 (1)
Co(2)–S(7)	2.313 (4)	S(7)–C(71)	1.77 (1)
Co(2)–S(8)	2.305 (4)	S(8)–C(81)	1.76 (1)
	$[(C_6H_5)_4P]_2[Co(SC_6H_5)_4]$[b]		
Co–S(1)	2.326 (4)	Co–S(3)	2.316 (4)
Co–S(2)	2.342 (4)	Co–S(4)	2.328 (4)

Selected Bond Angles (deg)

atoms	angles	atoms	angles
	$[(C_6H_{11})_2NH_2]_2[Co(SC_6H_5)_4]$[a]		
S(1)–Co(1)–S(2)	99.5 (1)	S(6)–Co(2)–S(8)	115.4 (1)
S(1)–Co(1)–S(3)	113.3 (1)	S(7)–Co(2)–S(8)	99.7 (1)
S(1)–Co(1)–S(4)	117.3 (1)	Co(1)–S(1)–C(11)	109.9 (4)
S(2)–Co(1)–S(3)	120.4 (1)	Co(1)–S(2)–C(21)	110.6 (4)
S(2)–Co(1)–S(4)	110.0 (1)	Co(1)–S(3)–C(31)	110.9 (4)
S(3)–Co(1)–S(4)	97.5 (1)	Co(1)–S(4)–C(41)	111.1 (4)
S(5)–Co(2)–S(6)	97.0 (1)	Co(2)–S(5)–C(51)	109.7 (4)
S(5)–Co(2)–S(7)	112.3 (1)	Co(2)–S(6)–C(61)	111.7 (4)
S(5)–Co(2)–S(8)	117.7 (1)	Co(2)–S(7)–C(71)	108.6 (4)
S(6)–Co(2)–S(7)	115.8 (1)	Co(2)–S(8)–C(81)	110.6 (4)
	$[(C_6H_5)_4P]_2[Co(SC_6H_5)_4]$[b]		
S(1)–Co–S(2)	95.6 (2)	S(2)–Co–S(4)	116.1 (2)
S(3)–Co–S(4)	97.0 (2)	S(1)–Co–S(4)	114.8 (2)
S(1)–Co–S(3)	121.3 (2)	S(2)–Co–S(3)	113.5 (2)
		Co–S–C(av)	109.9 (2.2)

[a] This work. [b] Reference 11.

Table III. Metal–Thiolate Stretching Modes

	T_2 (cm^{-1})	A_1 (cm^{-1})
$[(CH_3)_4N]_2[Fe(SC_6H_5)_4]$	229, 220	
$[(CH_3)_4N]_2[Co(SC_6H_5)_4]$	235, 228, 220	201
$[(C_2H_5)_4N]_2[Co(SC_6H_5)_4]$	234, 231, 217	
$[(C_6H_5)_4P]_2[Co(SC_6H_5)_4]$	235, 222, 214	
$[(CH_3)_4N]_2[Ni(SC_6H_5)_4]$	220, 211	
$[(CH_3)_4N]_2[Zn(SC_6H_5)_4]$	210, 199	202
$[(CH_3)_4N]_2[Co(SC_6H_4CH_3)_4]$	222	
$[(CH_3)_4N]_2[Zn(SC_6H_4CH_3)_4]$	185	
$[(C_6H_{11})_2NH_2]_2[Co(SC_6H_5)_4]$		192
$[(C_6H_{11})_2NH_2]_2[Zn(SC_6H_5)_4]$		180

Selection Rules. Assuming tetrahedral microsymmetry in $M(SC_6H_5)_4^{2-}$ compounds, four M–S vibrational modes are expected to occur with A_1(R), $2T_2$(R, IR), and E(R) representations, where R and IR denote Raman and infrared activity, respectively. Under D_2 symmetry, which can reasonably be applied to these compounds, the A_1 mode does not split; the T_2 vibrational mode splits into B_1(R, IR) + B_2(R, IR) + B_3(R, IR) modes, and the E mode splits into $2A$(R) modes. The T_2 modes, or those related to them in lower symmetry, are the only ones that should be observable by infrared spectroscopy.

Far-IR Metal–Ligand Frequencies. The far-IR spectra of $[(CH_3)_4N]_2[M(SC_6H_5)_4]$ complexes, M = Fe^{2+}, Co^{2+}, Ni^{2+}, Zn^{2+} (**4–7**), show variations in peak positions in the region 240–195

(10) Hamilton, W. C.; Ibers, J. A. *Hydrogen Bonding in Solids*; Benjamin: New York, 1968; Chapter 5.
(11) Swenson, D.; Baenziger, N. C.; Coucouvanis, D. *J. Am. Chem. Soc.* **1978**, *100*, 1932–1934.
(12) Kamata, M.; Hirotsu, K.; Higuchi, T.; Kido, M.; Tatsumi, K.; Yoshida, T.; Otsuka, S. *Inorg. Chem.* **1983**, *22*, 2416–2424.
(13) Harris, S. *Polyhedron* **1989**, *8*, 2843–2882.

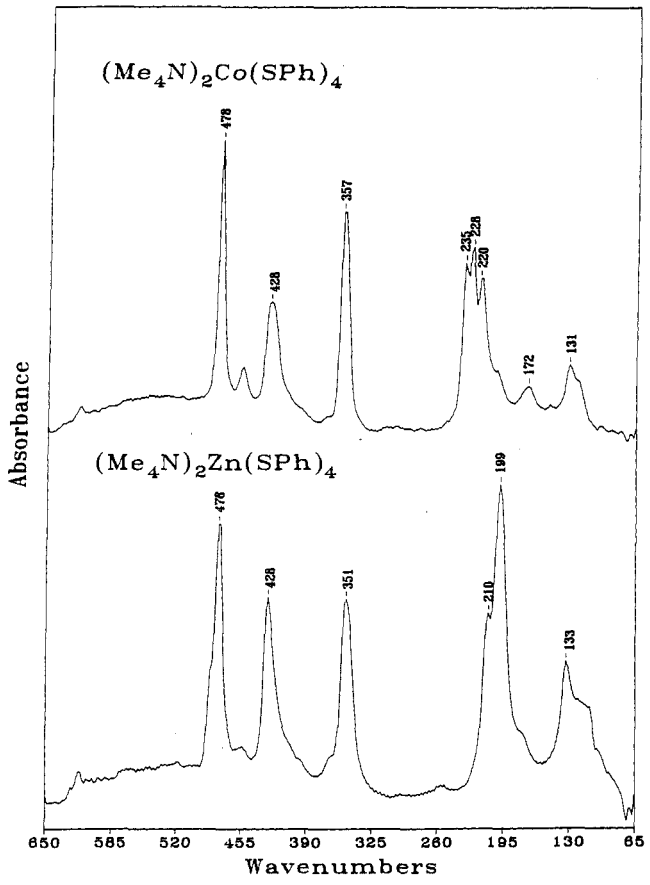

Figure 2. FTIR spectra of $[Me_4N]_2[Co(SPh)_4]$, (Me = CH_3, SPh = SC_6H_5) and $[Me_4N]_2[Zn(SPh)_4]$. The data shown represent the average of 600 scans.

cm^{-1} (Table III). The triplet centered at 228 cm^{-1} in $[(CH_3)_4N]_2[Co(SC_6H_5)_4]$ (**5**) apparently shifts to lower frequency with increasing central atom Z along the first-row transition-metal series, terminating with a doublet at 210 and 199 cm^{-1} in the Zn complex, **7** (Figure 2). In the cobalt *p*-thiocresolate complex $[(CH_3)_4N]_2[Co(SC_6H_4CH_3)_4]$ (**8**) the 228-cm^{-1} band is replaced by a broad singlet at 222 cm^{-1} (Table III). In the analogous Zn complex, **9**, this band is absent, and the corresponding band appears at 185 cm^{-1}. On the basis of the sensitivity of this band to the mass of the central metal and the effective ligand mass, it is assigned to a metal–ligand mode. More precisely it is probably an asymmetric stretching T_2 mode (assuming T_d symmetry) or a composite of $B_1 + B_2 + B_3$ modes congruent with the D_2 symmetry of the complex.

The T_2 asymmetric bending mode likely occurs in the vicinity of 130 cm^{-1}. A broad band is observed in that region. It is not as sensitive to metal ion Z as the higher frequency band. Our assignment for the metal–ligand stretch of compounds **4**–**7** agrees with that of Ueyama and co-workers[8] who characterized a series of complexes $[(CH_3)_4N]_2[M(XC_6H_5)_4]$, M = Zn, Cd, and X = S, Se, by X-ray diffraction and Raman and IR spectroscopy. They assigned a band at 198 cm^{-1} to a Zn–S vibration. Further support for the assignment of this series of bands is the fact that they shift, as a function of the central metal, in a similar manner as the ν_3 band of the series of first-row transition-metal tetrachlorides (Table IV).

In the hydrogen-bonding complexes **1** and **3**, plausible metal–ligand vibrational bands are observed in the region below 250 cm^{-1}. A peak is observed at 195 cm^{-1} in **1** which shifts to 179 cm^{-1} in the spectrum of **3** (Figure 3). Deuteration of the counterion to form **2** causes an apparent shift from 206 to 200 cm^{-1} of an unassigned band which occurs only as a shoulder in IR absorption data but is observed clearly in second derivative spectra (Figure 3). There are however no shifts in bands which are candidates for assignment to metal–ligand modes. Several

Table IV. Metal–Chloride Far-IR Asymmetric Stretching Bands

	T_2 (cm^{-1})		T_2 (cm^{-1})
$FeCl_4^{2-}$	283[a]	$NiCl_4^{2-}$	294, 280[b]
$CoCl_4^{2-}$	297[a]	$ZnCl_4^{2-}$	277[c]

[a] This work. Syntheses were performed by previously described methods: (i) Gill, N. S.; Nyholm, R. S. *J. Chem. Soc.* **1959**, 3997–4007. (ii) Gill, N. S. *J. Chem. Soc.* **1961**, 3512–3515. [b] Reference 24. [c] Reference 25.

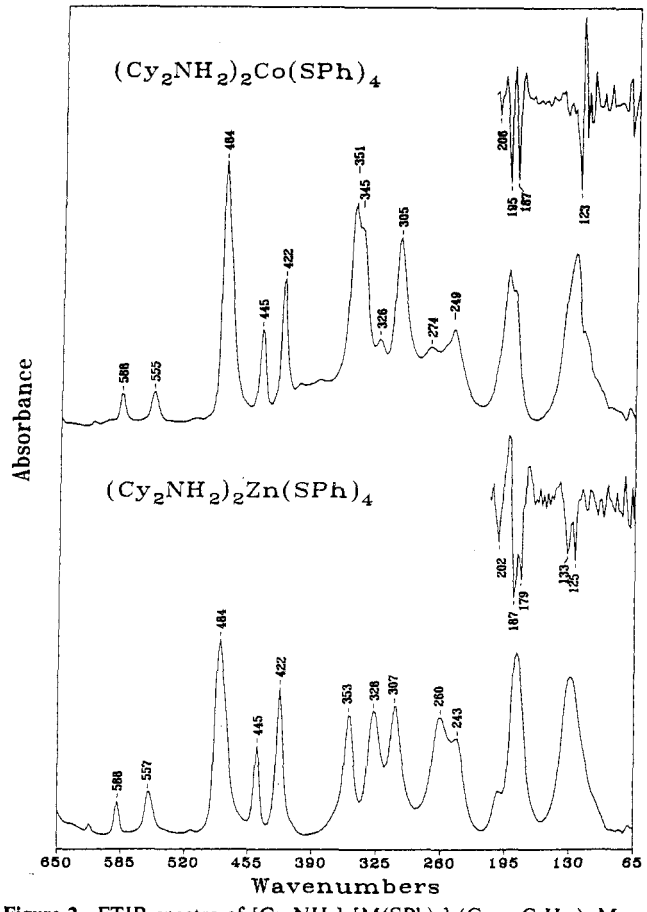

Figure 3. FTIR spectra of $[Cy_2NH_2]_2[M(SPh)_4]$ (Cy = C_6H_{11}), M = Co (top), Zn (bottom). Low-frequency peaks are resolved in the form of second derivatives, shown above corresponding IR absorption bands.

bands above 300 cm^{-1} shift appreciably, likely due to changes in the internal modes of the counterion.

The nature of the counterion can affect the geometry of ligand binding as has been shown for the tetrahedral complexes $[(C_6H_5)_4P]_2[Fe(SC_6H_5)_4]$ and $[(C_2H_5)_4N]_4[Fe(SC_6H_5)_4]$.[14] Differences in conformation may account for the frequency shifts in the Co–S "T_2" stretch between the IR spectra of $[(C_6H_5)_4P]_2[Co(SC_6H_5)_4]$, $[(CH_3)_4N]_2[Co(SC_6H_5)_4]$, and $[(C_2H_5)_4N]_2[Co(SC_6H_5)_4]$. For these compounds the putative Co–S bands occur at 235, 222, 214; 235, 228, 220; and 234, 231, 217 cm^{-1}, respectively (Table III). The spectroscopic features of these compounds are distinctly different from those of the hydrogen-bonded system $[(C_6H_{11})_2NH_2]_2[Co(SC_6H_5)_4]$ (**1**). Thus it is expected that in the latter complex, hydrogen bonding and its effect on the symmetry of the complex exerts a sizable effect on the frequencies of the metal–ligand vibrational modes.

Raman Metal–Ligand Frequencies. The band centered at 228 cm^{-1} in **5** is not observed in the Raman spectrum of the complex by using argon ion laser excitation in the range 457.9–514.5 nm. A band is observed, however, at 201 cm^{-1} which shows evidence of a weak resonance enhancement with 514.5-nm radiation and diminishes in its relative intensity at shorter excitation wavelengths (Figure 4a). Because of its resonance enhancement and position

(14) Swenson, D. Ph.D. Thesis, University of Iowa, 1979.

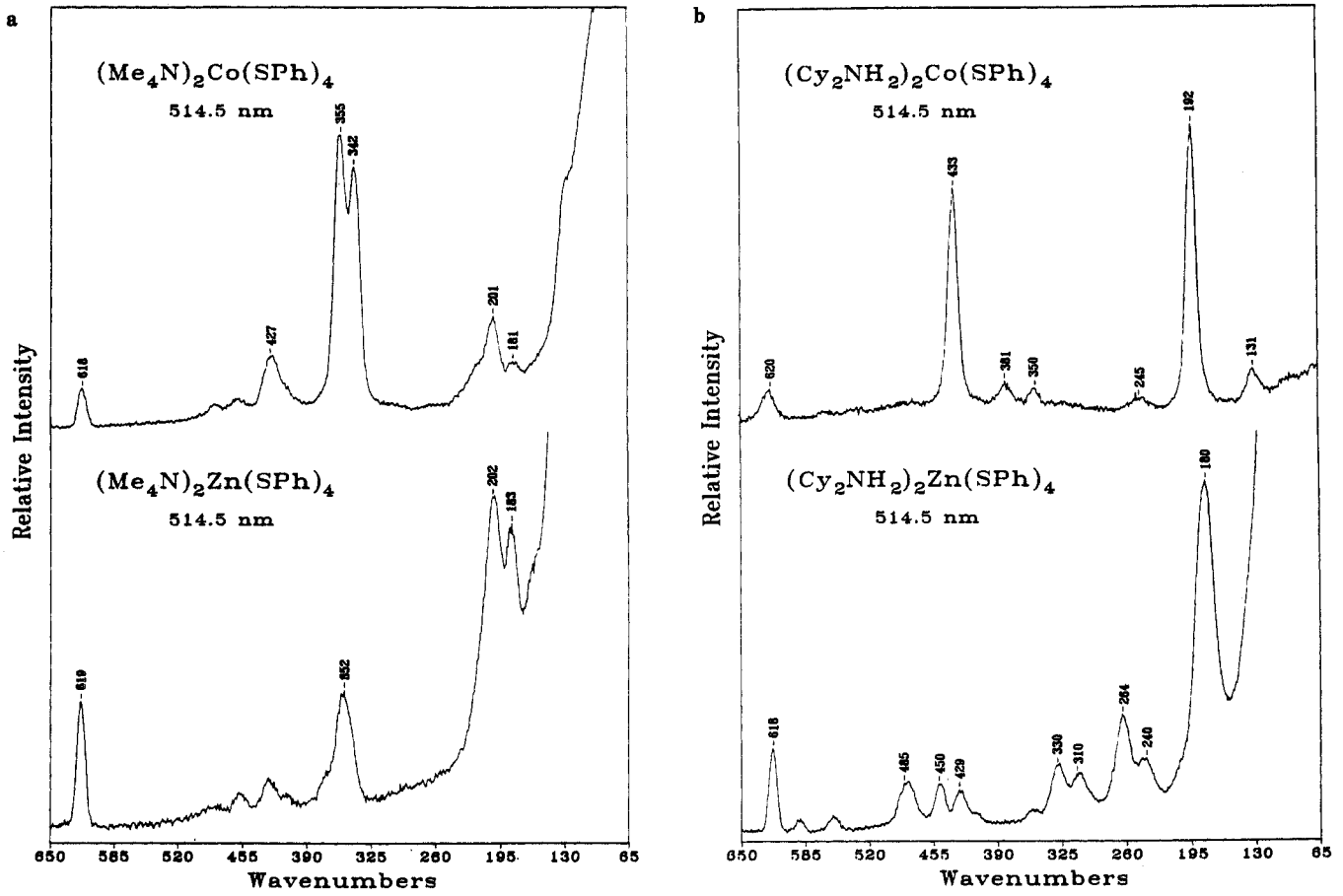

Figure 4. (a) Raman spectra of $[Me_4N]_2[M(SPh)_4]$, M = Co (top), Zn (bottom). (b) Raman spectra of $[Cy_2NH_2]_2[M(SPh)_4]$, M = Co (top), Zn (bottom).

between the two putative T_2 modes of the complex it is a plausible candidate for the A_1 mode. In the Raman spectrum of **1** a very intense band appears at 192 cm^{-1} which is assigned to the A_1 stretch in the hydrogen-bonded complex (Figure 4b). In the Zn complex, **7**, bands are observed at 202 and 183 cm^{-1} (Figure 4a). The former is assigned to the A_1 mode. The latter is probably due to a phenyl ring out-of-plane mode.[15,16] In the hydrogen-bonded Zn complex a strong Raman band is observed at 180 cm^{-1} and is tentatively assigned to the A_1 stretch (Figure 4b). According to our assignments hydrogen bonding causes the A_1 mode to shift by −9 cm^{-1} in the Co complex and −22 cm^{-1} in the Zn complex.

In Raman spectroscopic studies of $[(C_6H_5)_4P]_2[Co(SC_6H_5)_4]$ Salama et al.[17] assigned a band at 192 cm^{-1} to the Co–S A_1 mode. Such an assignment would suggest that this band undergoes no shift as a result of hydrogen bonding. This interaction however is known to cause a decrease of 0.02 Å in the average metal–ligand bond length. A change of equal magnitude is likely for the Zn complex. From the application of Badger's rule[18] a frequency *upshift* of about 5 cm^{-1} is predicted. The apparent frequency decreases observed in the Co–S stretches may be due to a change in the nature of the normal modes as a result of hydrogen bonding or perhaps strong internuclear coupling of metal–ligand vibrations in the one-dimensional concatenated arrangement of cobalt–thiolate complexes.

Mid-IR Ammonium N–H Frequencies. In the mid-IR spectrum of **1** a broad manifold of bands is observed over the range 2787–2343 cm^{-1}. This feature is characteristic of the ν(N–H) stretching frequencies of secondary ammonium anions.[19] The occurrence of a manifold of N–H bands for alkylammonium ions in the solid state has been attributed to the nonadiabatic coupling of the N–H modes to the low-frequency N···L hydrogen bond mode, internal C–H modes of the ligand, and phonons.[20] As a result of relatively strong hydrogen bonds, the bands are shifted lower in frequency and intensity, relative to those of dicyclohexylammonium chloride which exhibits a manifold of bands in the range 2796–2361 cm^{-1} (Figure 5).

Our mid-IR spectra can be compared with the results of Kristof and Zundel[21] who reported on hydrogen bonding between polycysteine and polylysine. They suggest that the limiting structures N···H–S, and N–H···S have equal weight. In such a system proton transfer is facile, and the proton is highly delocalized in a broad molecular potential. This would explain the appearance of a broad ν(N–H) absorption continuum in the range 2900–1700 cm^{-1}. This is characteristic of long easily polarizable proton-transfer hydrogen bonds.[22] We do not observe a comparable continuum absorption in the spectrum of **1** and must presume that proton transfer does not occur and that the hydrogen bond in this complex salt is less polarizable.

Electronic Absorption Spectra. Because hydrogen bond interaction is disrupted in solution, electronic absorption data of **1** and **5** were recorded with the complexes dispersed in KBr pellets in amounts of 0.05 wt %. Absorption maxima were observed at 654 (15 291 cm^{-1}), 692 (14 451 cm^{-1}), and 746 (13 405 cm^{-1}) nm in **5**, characteristic of Co(II) d–d transitions. Spectra have previously been reported for **5** in solution by Dance,[7] with bands

(15) Dollish, F. R.; Fateley, W. G.; Bentley, F. F. *Characteristic Raman Frequencies of Organic Compounds*; Wiley: New York, 1974; pp 162–175, and references therein.
(16) Scherer, J. R. *Spectrochim. Acta* **1968**, *24A*, 747–770.
(17) Salama, S.; Schugar, H.; Spiro, T. G. *Inorg. Chem.* **1979**, *18*, 104–107.
(18) Herschbach, D. R.; Laurie, V. W. *J. Chem. Phys.* **1961**, *35*, 458–463.
(19) Nakanishi, K.; Goto, T.; Ohashi, M. *Bull. Chem. Soc. Jpn.* **1957**, *30*, 403–408.
(20) Hadzi, D.; Bratos, S. In *The Hydrogen Bond*; Schuster, P., Zundel, G., Sandorfy, C., Eds.; North Holland: Amsterdam, 1976; Vol. II, Chapter 12, and references therein.
(21) Kristof, W.; Zundel, G. *Biopolymers* **1982**, *21*, 25–42.
(22) Zundel, G. In *The Hydrogen Bond*; Schuster, P., Zundel, G., Sandorfy, C., Eds.; North Holland: Amsterdam, 1976; Vol. II, Chapter 15.

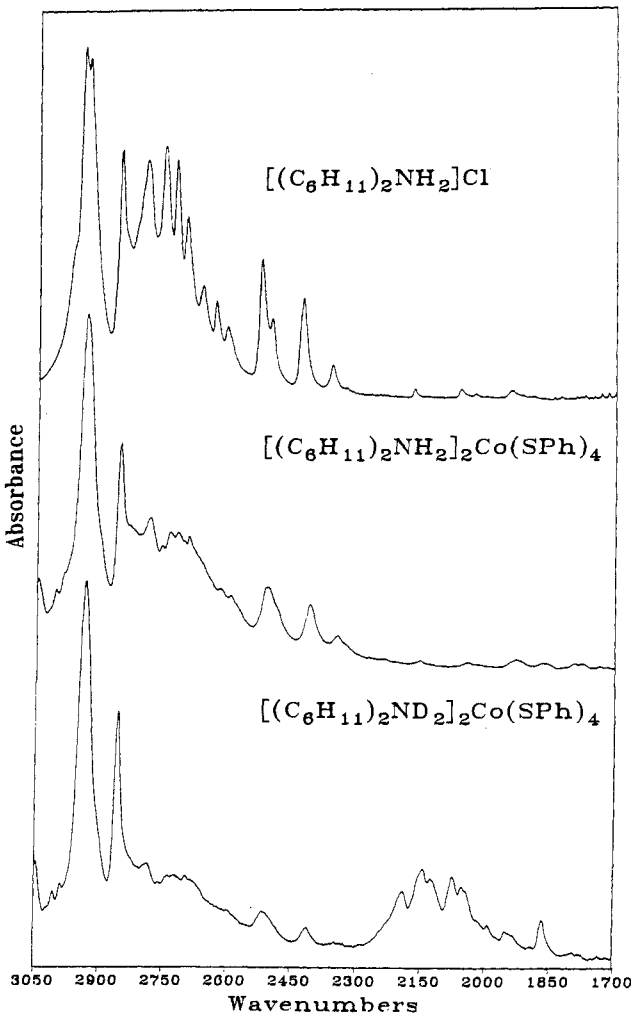

Figure 5. Spectra of $[(C_6H_{11})_2NH_2]Cl$ (top), $[(C_6H_{11})_2NH_2]_2[Co(SPh)_4]$ (middle), and $[(C_6H_{11})_2ND_2]_2[Co(SPh)_4]$ (bottom). The spectra shown are the averages of 60 scans.

appearing at 625, 693, and 734 nm, and by Swenson et al.[11] with bands at 635, 690, and 730 nm. In **1** a peak is observed at 702 (14 245 cm^{-1}) nm with shoulders at 606 (16 502 cm^{-1}) and 740 (13 514 cm^{-1}) nm. These three bands belong to the transition $A_2 \rightarrow T_1(P)$ of a tetrahedral complex. Similar band splitting in the spectra of Co halide complexes has been ascribed to excited-state dynamic Jahn–Teller effects.[23] On the basis of the negligible shift in the center of gravity of the $A_2 \rightarrow T_1(P)$ transition in **1** and **5**, hydrogen bonding appears to have little effect on the magnitude of the thiolate ligand field. Charge-transfer (CT) bands in **1** and **5** appear as broad shoulders at 420 nm. A CT band has previously been reported at 420 nm for **5** in solution.[11]

Conclusion. In the series of experiments reported here we provide the first structural details on N–H···S hydrogen-bonding interactions in a metal complex. We observe a 0.02-Å decrease in the average Co–S bond length relative to that reported for the analogous non-hydrogen-bonded complex. The results suggest that such interactions could stabilize the structure of metal-binding sites in metallothionein. This should provide a useful reference for the characterization of similar hydrogen-bonding interactions in metallothionein and other metalloproteins which involve the coordination of metal ions by Cys. The hydrogen bond distances found in **1**, which average 3.29 Å, are indicative of strong bonding relative to known N–H···S interactions. In metallothionein seven Lys–Cys interactions are insufficient to provide individual hydrogen bonds to each of the Cys ligands but could serve to neutralize the cluster charges of the α and β domains. Accordingly, it can be expected that the metal–ligand bonds would be stabilized by hydrogen bonding to a lesser degree than in the model complexes discussed here.

Acknowledgment. We thank Dr. L. Noodleman, Prof. J. Sanders-Loehr, and Prof. T. G. Spiro for helpful discussions. We also thank Mr. B. Bowen for the synthesis of $[(C_2H_5)_4N]_2[Co(C_6H_5)_4]$. This research was supported by contract DHHS/BRSG 2 S07 RR07062 to M.A.W.

Note Added in Proof. Recent results from the laboratory of Dr. C. D. Stout have substantiated the occurrence of N–H···S hydrogen bonding in metallothionein (private communication). This involves both lysine $-NH_3^+$ and amide –NH as donor groups, with the latter predominating. it is expected that the results reported in this work on Cy_2NH_2–SPh interactions will be generally applicable to an understanding of the hydrogen bonding effects of ammonium or amide donor groups.

Registry No. 1, 130574-91-3; **2**, 130574-94-6; **3**, 130574-96-8; **4**, 87482-70-0; **5**, 72061-33-7; **6**, 130575-01-8; **7**, 76915-22-5; **8**, 130574-98-0; **9**, 130575-00-7; **10**, 4693-92-9; $[(C_6H_5)_4P]_2[Fe(SC_6H_5)_4]$, 57763-34-5; $[(C_2H_5)_4N]_2[Co(SC_6H_5)_4]$, 72043-41-5; $[(C_6H_5)_4P]_2[Co(SC_6H_5)_4]$, 57763-37-8; $[(C_6H_5)_4P]_2[Ni(SC_6H_5)_4]$, 57927-74-9; $[(C_6H_5)_4P]_2[Zn(SC_6H_5)_4]$, 57763-43-6; $[(C_2H_5)_4N]_2[Ni(SC_6H_5)_4]$, 93841-89-5; $[(C_2H_5)_4N]_2[Zn(SC_6H_5)_4]$, 93714-75-1; L-lysine, 56-87-1; L-cysteine, 52-90-4; dicyclohexylamine, 101-83-7; benzenethiol, 108-98-5; cobalt(II) chloride hexahydrate, 7791-13-1; sodium benzenethiolate, 930-69-8; zinc chloride, 7646-85-7; dicyclohexylammonium chloride, 4693-92-9.

Supplementary Material Available: General structure report for compound **1**, including details of the structure determination, listings of experimental details, positional and thermal parameters, inter- and intramolecular distances and bond angles involving non-hydrogen atoms, and intermolecular distances involving hydrogen atoms, and ORTEP and PLUTO drawings of the structure (81 pages); a listing of final observed and calculated structure factors (45 pages). Ordering information is given on any current masthead page.

(23) Cotton, F. A.; Goodgame, D. M. L.; Goodgame, M. *J. Am. Chem. Soc.* **1961**, *83*, 4690–4699.
(24) Edwards, H. G. M.; Woodward, L. A.; Gall, M. J.; Ware, M. J. *Spectrochim. Acta* **1970**, *26A*, 287–290.
(25) Avery, J. S.; Burbridge, C. D.; Goodgame, D. M. L. *Spectrochim. Acta* **1968**, *24A*, 1721–1726, and references therein.